

Chapter 5: Reservoir Characterization

Introduction

Understanding the porous media within shale rock is crucial to determine the gas storage capacity and gas flow within it. Analytical technologies at the microscopic level enable to understand the rock properties and petrophysical characteristics. This chapter deals with the evaluation of the reservoir characteristics of Barren Measures shale using helium porosimetry, air permeability, advanced imaging techniques like Scanning Electron Microscopy (SEM), Micro Computer Tomography (μ CT) and Transmission Electron Microscopy (TEM) to envisage multiscale pore system, pore structure in the clay and organic matter (OM) components within Barren Measures shale.

The pore-shapes influence the behavior of porous media, i.e., elastic and mechanical behavior, movement and flow of fluids etc. Understanding and quantification of pore-structure parameters is vital in modeling behavior of porous media, however, smaller pores have large specific surface areas and nano pore typically possess larger specific surface areas. Natural gas can be adsorbed on these internal surfaces contributing to gas storage capacity in the shale. Therefore, specific surface area measurement along with pore size distribution was carried out using BET. It is expressed as surface area per unit mass of sample or 'specific surface area'. The external sample specific surface areas of shale are lesser in comparison to that on the 'internal' pore wall.

Helium Porosimetry

The Helium Porosimetry results very low effective porosity of the Barren Measures shales ranging from 0.02 to 1.347%. The air permeability of 13 samples was analysed and observed 0 to 0.18 md permeability. The average porosity and permeability were obtained as 0.633% and 0.135 md respectively. The results of helium Porosimetry and air permeability were tabulated below (Table 5.1). It has been difficult to determine porosity of the shale using He Porosimetry as the pores are fine, isolated and much smaller than conventional reservoir rock i.e. sandstone and carbonates. It is a complex phenomenon to determine accurate porosity and permeability in conventional laboratory conditions at low pressure (400psi).

Table 5.1: Results of helium porosimetry, grain density and air permeability

Boreholes	No	Depth (m)	Porosity %	Grain Density (g/cc)	Air Permeability (md)
BOREHOLE#1	1	150	1.104	2.51	NC
	2	155	0.9	2.40	0.156
	3	170	0.95	2.40	NC
	4	185	0.546	2.41	0.167
	5	195	0.474	2.41	0.144
BOREHOLE#2	1	90	0.959	2.56	0.18
	2	96	1.055	2.57	0.12
	3	100	1.347	2.52	NC
	4	115	0.014	2.53	0.15
	5	150	1.02	2.52	0.11
	6	155	0.8	2.40	0.148
BOREHOLE#3	1	110	0.972	2.50	0.167
	2	115	1.211	2.55	NC
	3	120	0.366	2.46	0.164
	4	125	0.129	2.45	0.162
	5	154	0.02	3.08	0.122
BOREHOLE#4	1	305	0.08	2.45	0.1
	2	315	0.09	2.48	0.0
	3	320	0	3.09	NC

* NC=not calculated

Air Permeability Measurement

Air permeability has been determined using Ultraperm 400 based on Darcy's law (Chalmers *et al*, 2012; Heller *et al*, 2014). Measurement of permeability in low permeability shales like Barren measures is very difficult by using the conventional laboratory condition, which results very low permeability. Most of the samples of lower permeability, equilibrium was not reachable in a reasonable amount of time using steady-state methods, so permeability could not be measured for all samples. Although, the air permeability of 13 core samples were measured using conventional laboratory condition.

The plots of depth versus porosity (Figure 5.1A) and porosity versus permeability (Figure 5.1B) were interpreted to understand the compaction trend. Figure 5.2 shows the inverse relationships between grain density and porosity.

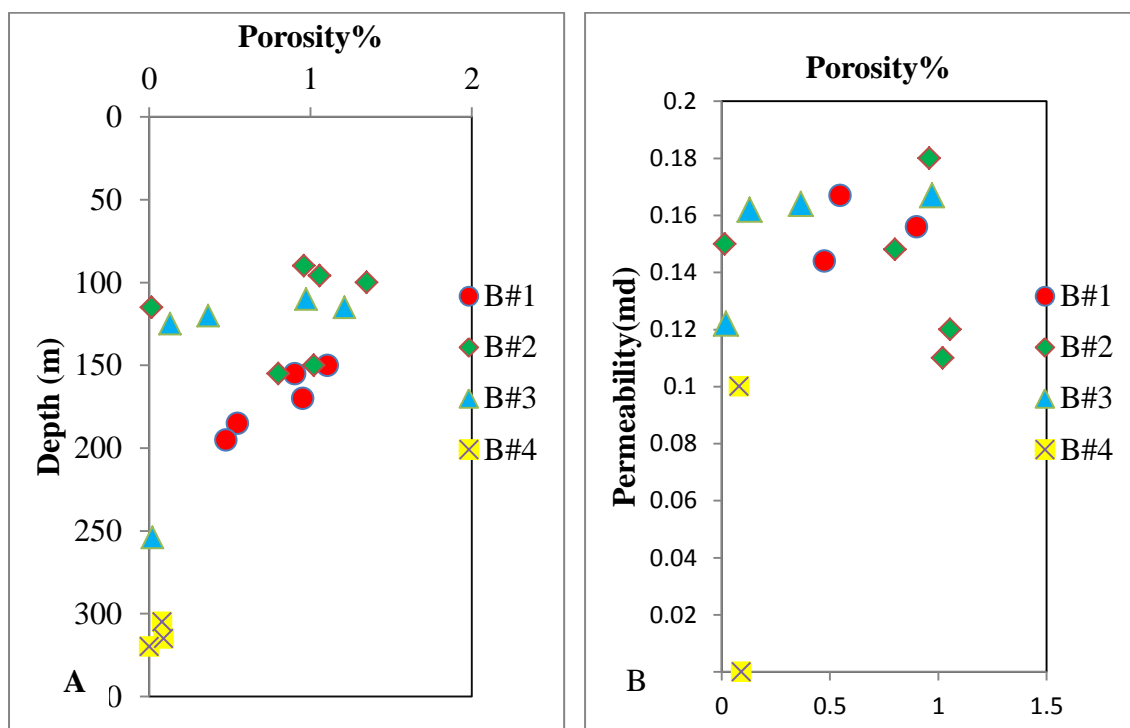


Figure 5.1 Plots of porosity and permeability measurement. A. Porosity with depth; B. Porosity and permeability relationship.

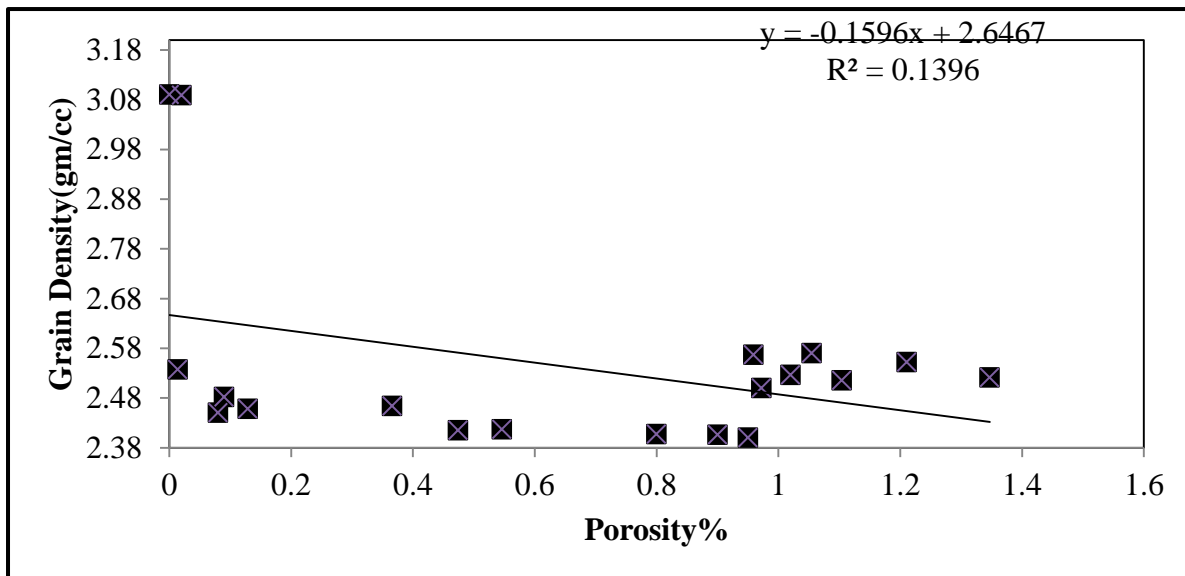


Figure 5.2 Grain density and Porosity relationship.

Scanning Electron Microscopy (SEM)

The sample preparation and analytical techniques of SEM are discussed in the Chapter 1. Based on SEM images the pores systems of Barren Measures shales are classified as: (a) intergranular pores (Plate 5.1A-D; 5.2A, B); (b) intragranular pores (Plate 5.2 C, D; 5.4 A, B); (c) secondary pores developed due to diagenesis, dissolution activities etc. (Plate 5.3A-D); (d) matrix pores and (e) pores associated with organic matter (Plate 5.4C; 5.5A-C). Organic flakes (compressed wood chips, leaf fragments, etc.) are observed lying parallel to bedding (Plate 5.4C). Pores are also developing due to presence of both natural and mechanical fractures (Plate 5.6A-D). EDX analysis of selective images also reveals the presence of organic matter (C) and iron rich matrix (Fe) (Plate 5.4D & 5.5D).

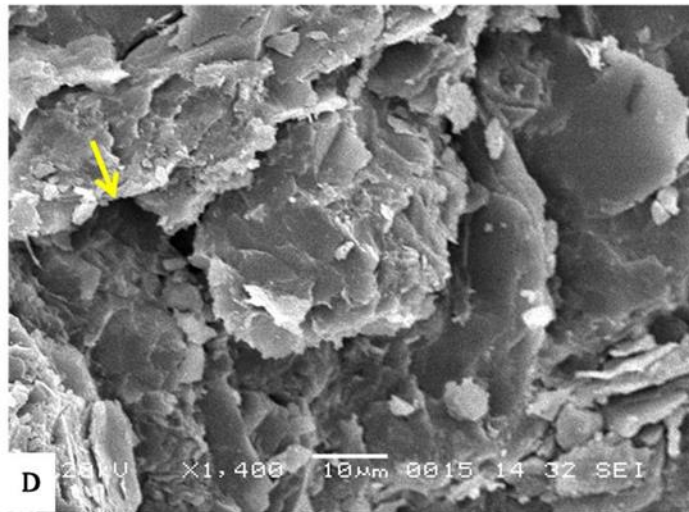
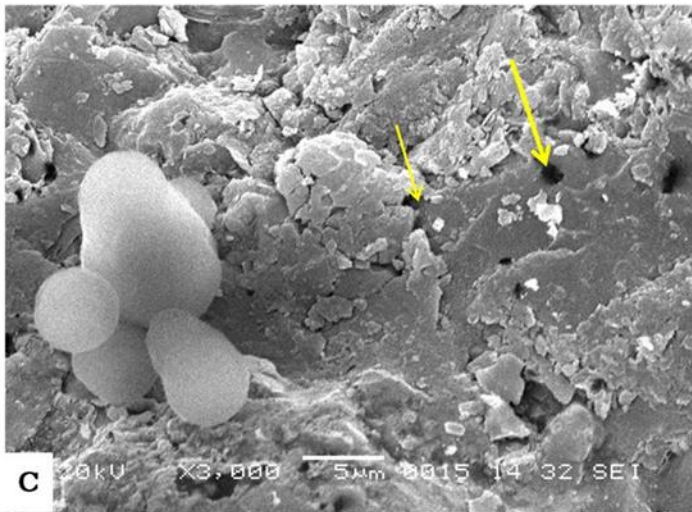
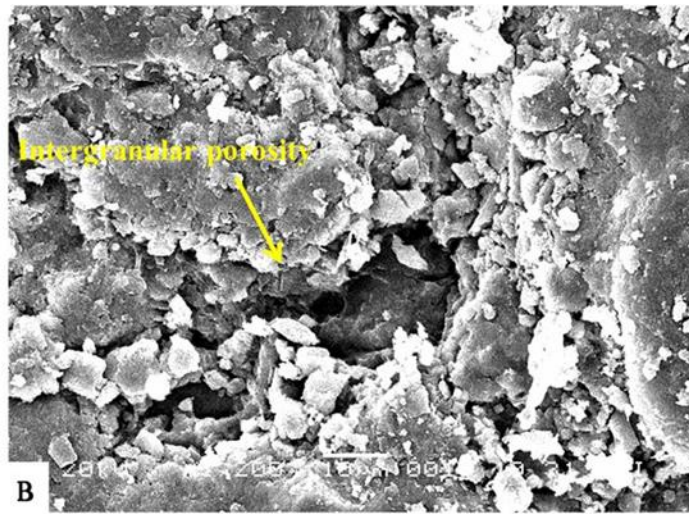
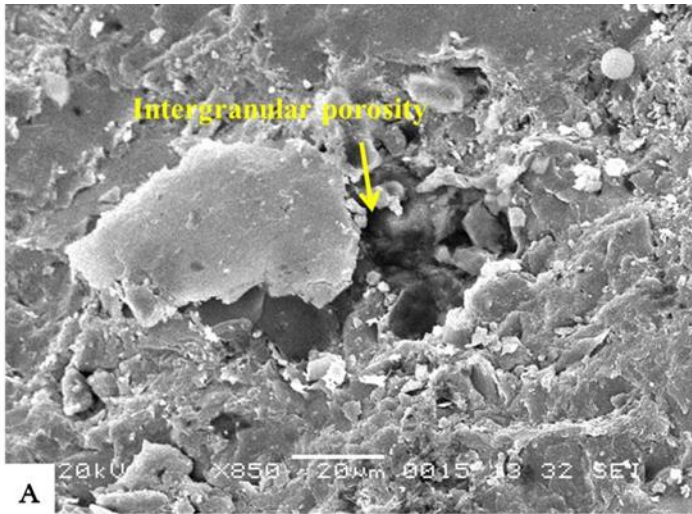


Plate 5.1 Photomicrograph of Primary (intergranular) pores in Barren Measures shale.

- A. *Intergranular pores partially filled with organic matter (185m; B#1).*
- B. *Intergranular pores (185m; B#1)*
- C. *Pores partially filled with organic matters;*
- D. *Intergranular pores (195m; B#1).*

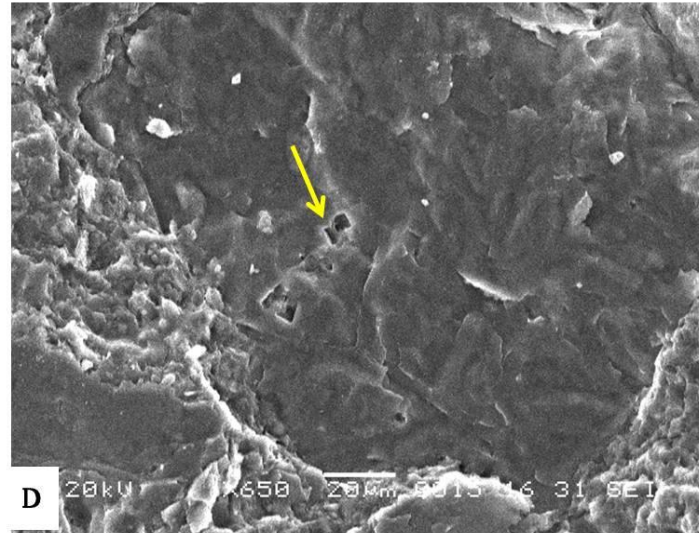
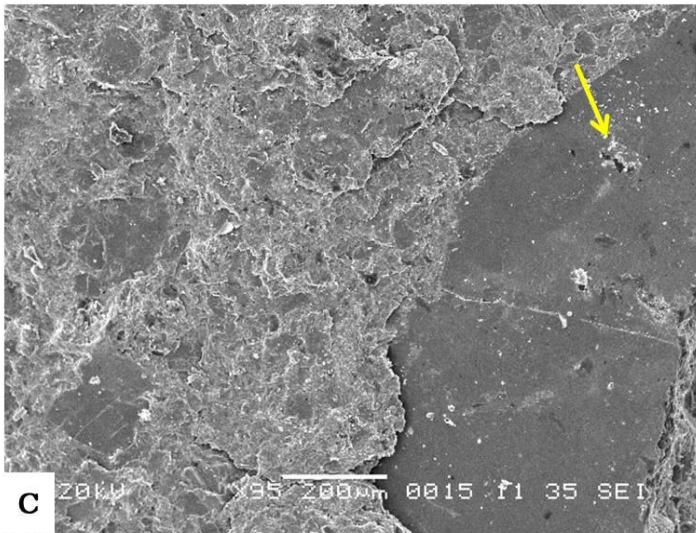
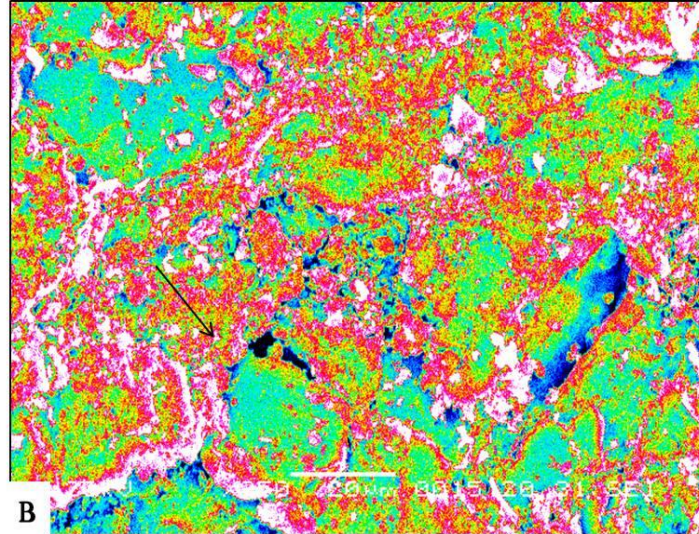
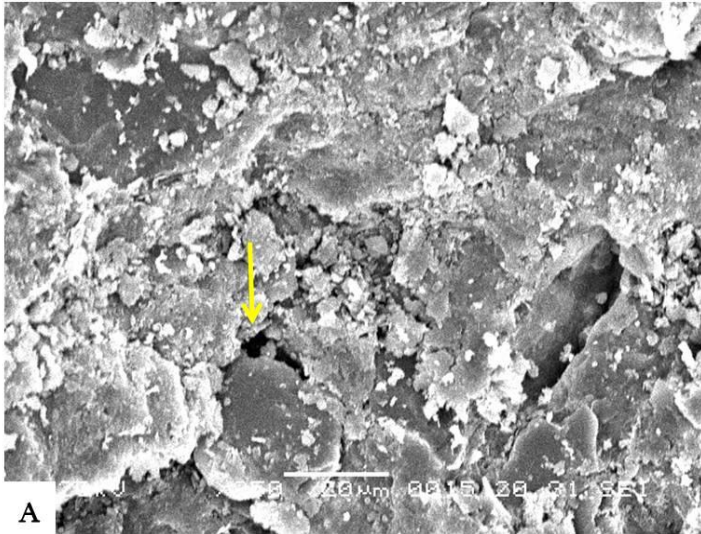


Plate 5.2. Photomicrograph of pore type in Barren Measures shale.

- A. *Intergranular pores(190m; B#1)*
- B. *Intergranular pores*
- C. *intragranular pores (147m; B#3)*
- D. *Intragranular pores(149m; B#3)*

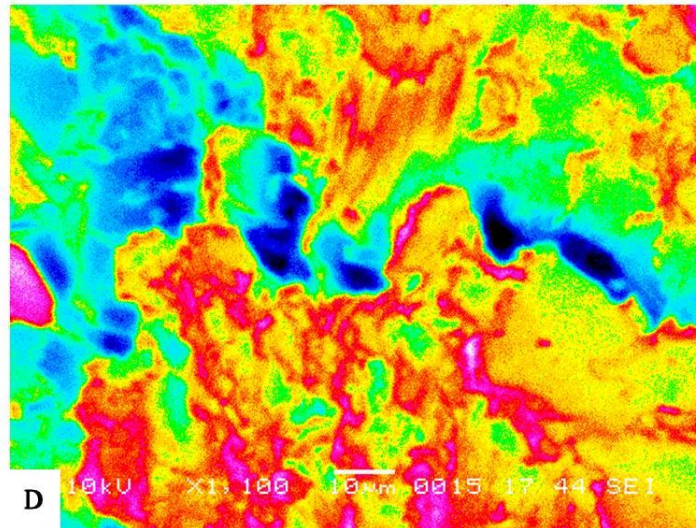
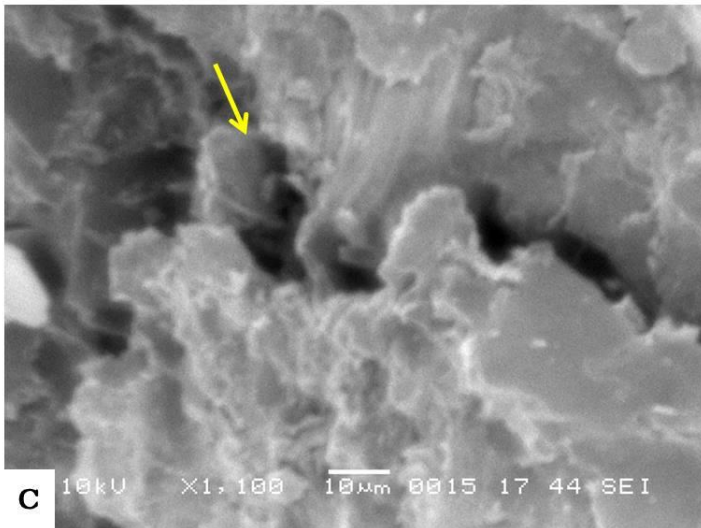
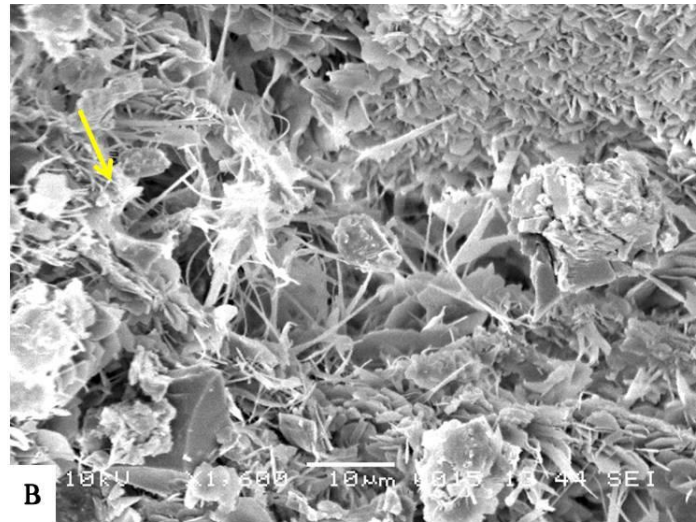
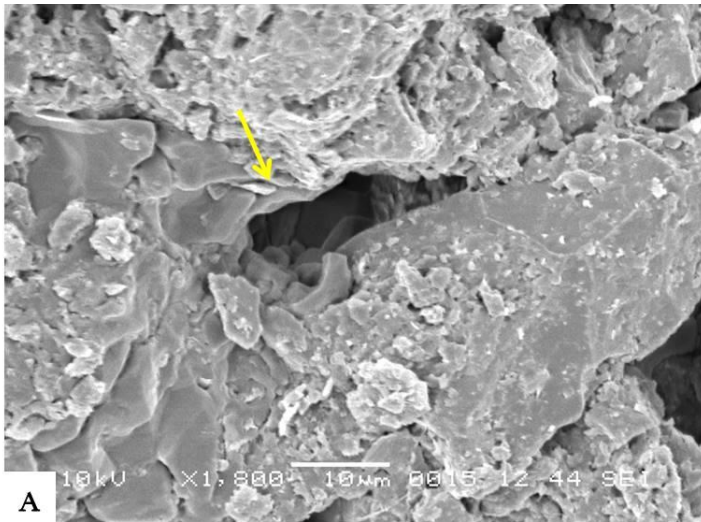


Plate 5.3 Photomicrograph of Secondary poros in Barren Measures shale.

- A. Pores due to dissolution activity(156m; B#3)
- B. Pores within clay(160m, B#3)
- C. Feldspar alteration is affecting the pore spaces (301m; B#4).
- D. Colour image of fig C, showing the pores in blue colour.

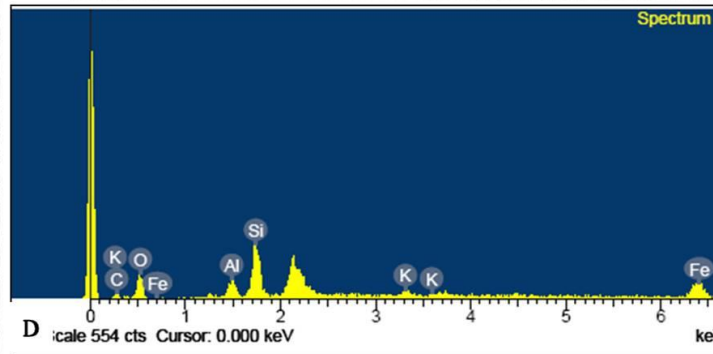
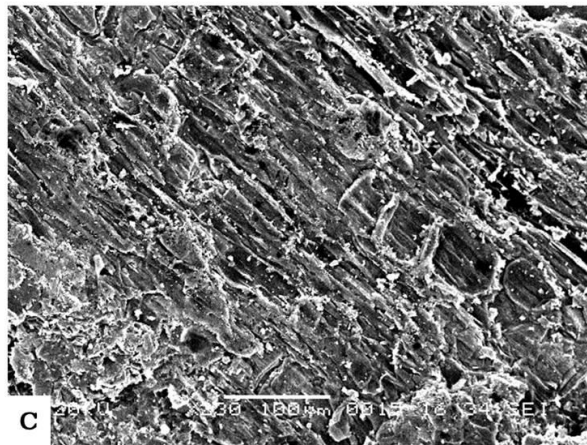
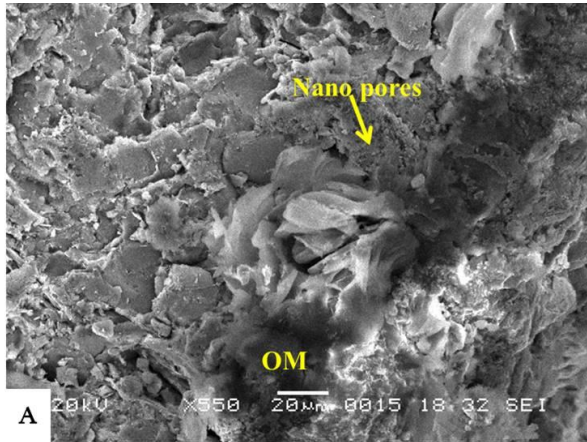


Plate 5.4 Both intragranular and matrix pores in Barren Measures shale.

- A. The rock matrix is clay rich and showing micro pores within the grain and on the surface. Depth interval 145-150m, borehole#1.
- B. pores are clearly seen in magnified scale of the same image;
- C. Organic matters are to be present like woody materials and micro pores are associated with OM.(170m; B#1)
- D. The EDX analysis of image A indicates the presence of K, Al, Si, O, Fe, C elements in the rock.

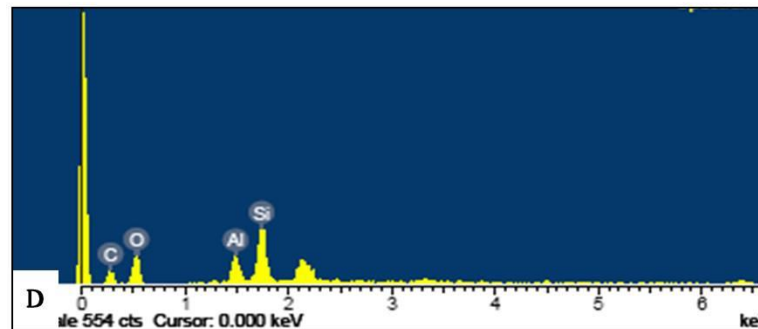
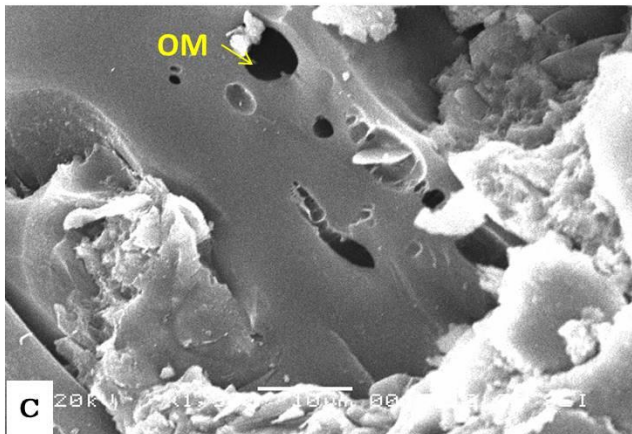
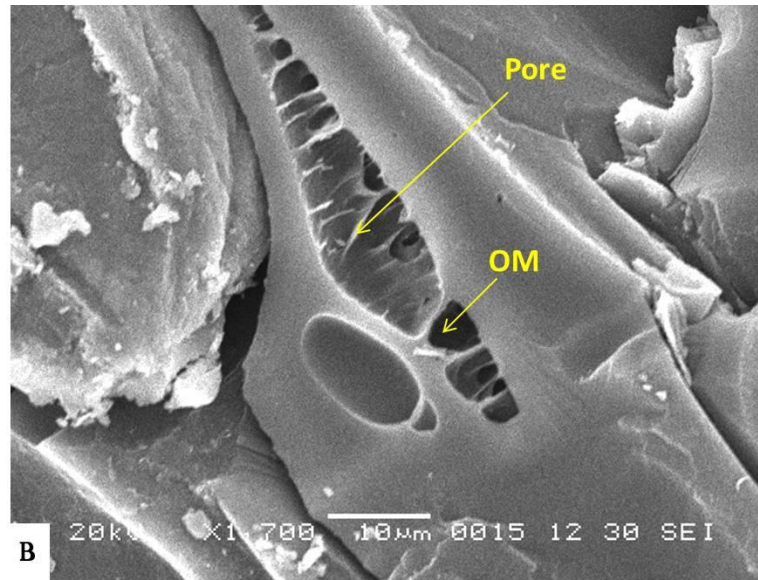
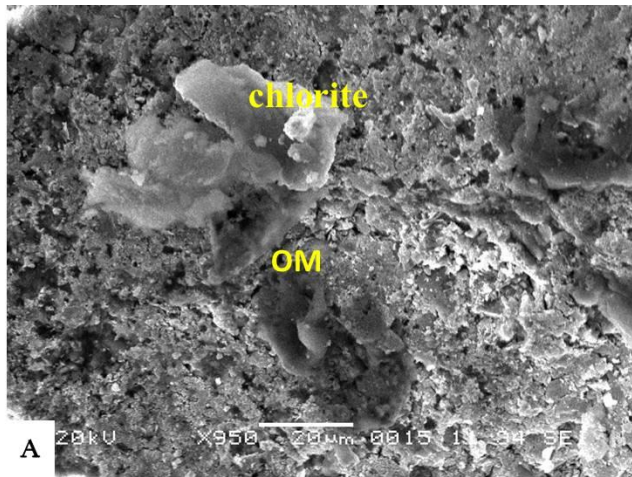


Plate 5.5 Pores associated with organic matter.

- A. Micro pores scattered on the rock surface ; (170m, B#2).
- B. Pores are developing due to dissolution of organic matter;
- C. Pores are partially filled with organic matter;
- D. EDX analysis shows the carbon (organic matter) rich rock surface.

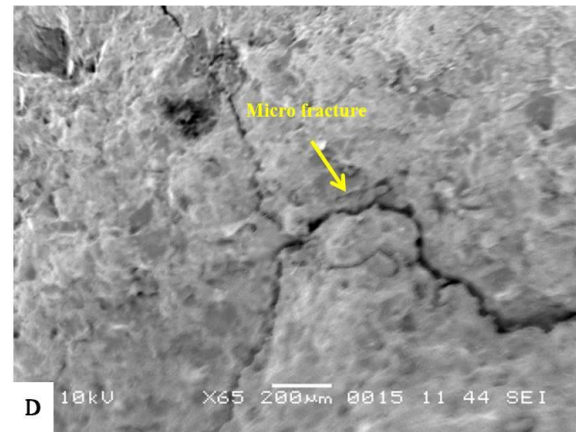
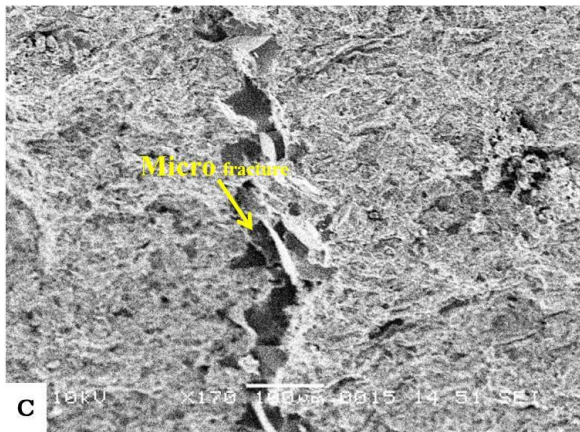
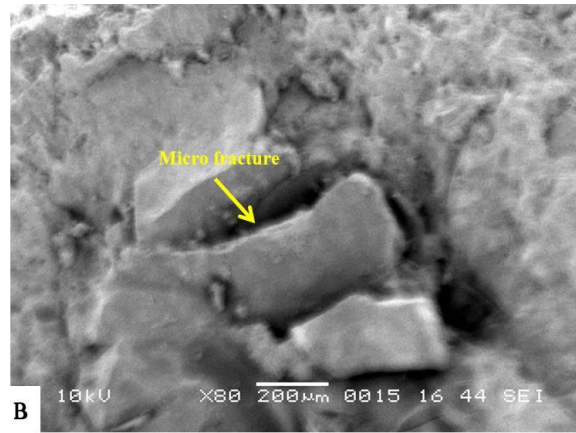
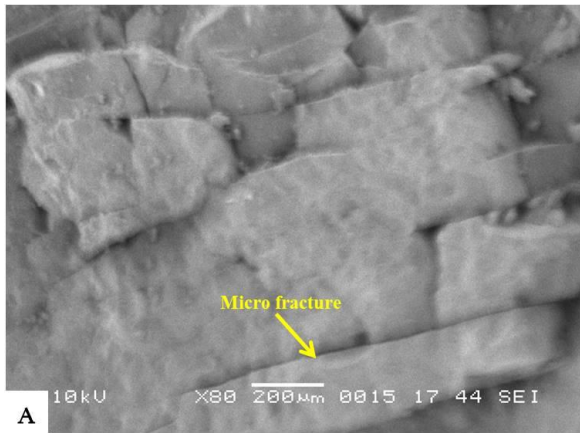


Plate 5.6 photomicrograph of highly fractured zone.

A, B. Cleats like micro fractures. Depth interval 141-144m; borehole#1;

C, D. Mechanical fracture. Mineral grains are covered by clay matrix. Depth 175-180m; borehole#1

Pore System Analysis by Micro Computer Tomography (μ CT)

Two subsamples of diameters 5mm from 155m and 155.1m depth and one subsample of 10mm from 185m depth zone of borehole B#1 were extracted perpendicular to the bedding using drill bit cutter of 5mm and 10mm respectively. The X-ray source generates polychromatic X-rays using a 30 – 225 kV/1mA electron beam with 2 micron minimum focal spot size (Resolution up to 2-3 micron). A rotation stage rotates the specimen during data collection with an accuracy of 1milli-degree. The X-ray Camera records the X-ray radiographs with an active area 70 x 70 mm² 16-bit pixels and a down load time of 1 Megapixel per second. The projection data are collected with cone beam geometry, the specimen rotated through full 360° (Figure 5.3). Optimal no. of projections, $N_o = (\pi/2) N_w$, where N_w is the no of pixels in the width of the detector.

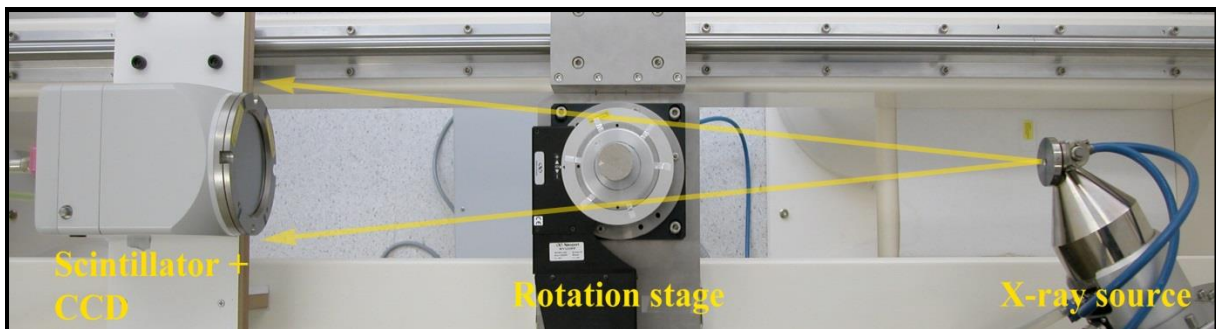


Figure 5.3 Experimental X-ray CT apparatus.

CT measures the linear attenuation coefficient μ . The linear attenuation coefficient is defined by Beer's law and it measures the fraction of X-rays that pass through the shale sample. The linear attenuation coefficient is related to other physical properties by

$$\mu = \rho_b (a + bZ^{3.8}/E^{3.2})$$

Where ρ_b = bulk density (electron density), a and b = constants, Z=effective atomic number, and E=X-ray energy. At low energies, μ will be primarily a function of Z; and at high

energies μ will be primarily a function of ρb (Taud *et al*, 2005; Yao *et al*, 2009; Golab *et al*, 2013).

The samples were dried and cleaned using acetone. For acquisition of image, the magnification was set by adjusting the ratio of the distance between the X-ray source and the specimen to the distance between the X-ray source and the camera. Images were acquired at 2048 voxels with and no. of projections was 2880. It produces a series of 2D images that are called “slices”. The projections were linearized and reconstructed using Feldkamp method in Q-MANGO (Medial Axis and Network Generation) software to get the tomogram (2048³ voxel size) images. These attenuation data are transformed to CT numbers, a function of density and effective atomic number of the investigated object that has a range determined by the computer system, (Shah *et al*, 2015).

The tomogram (3D representative of the rock) was segmented into two-phase (pore and grain) and three-phase (pore, grain and intermediate). Different noise reducing filters are applied before segmentation for better visualization of the tomogram. Image processing was run by Q-MANGO. The images were achieved by acquiring a series of radiographs at different viewing angles. These images were later piled together mathematically to produce virtual cut sections (multi-planar reconstruction) in the volume data set to show the inner heterogeneity. The shale is composed of pores, organic matter, matrix, and minerals and these components have a certain range of CT number, and they can be quantified by the threshold or segmentation method. The segmentation technique first defines an upper and a lower threshold of CT numbers for each component. Then the area with the CT numbers between the lower and upper thresholds is defined as the region of the component. Pores and grains in the tomogram image were differential by filling with blue, red and grey colours respectively. The porosity of the samples was calculated by segmentation thresholding techniques to segmented images. In shale rock, the geometry of cracks or pores spaces are more complex

and irregular, consequently the segmentation is more complex. The Digital Terrain Model (DTM) theory (Taud, 2005) was used to calculate porosity where CT image is symbolized as a Digital Terrain Model. The grey level in the DTM image is related to the altitude or elevation terrain. Based on system generated tentative values of pores and grains, segmented images were analysed with the help of Q-Mango software and pore network of the rock samples were extracted. 3D visualization of the pore-networks was visualized using Paraview software. Different filters like euclidean distance, smooth distance map, watershed transform, cluster region merging etc. were used to enhance the resolution quality of the tomogram images to analyse texture and the pore & pore throat network. There are commonly two methods for calculating porosity of rock using m CT images i.e. the dual scan and image segmentation methods. The present study used the segmentation method based on mathematic programme (Van *et al.*, 2000).

a. Identifying Pore and Mineral Phase Distributions

Micro-fractures, sorting of grains, grain size, presence of laminae, organic matters and pore distribution and micro scale heterogeneity were observed in the core samples using computer tomogram (m CT) images (Figure, 5.4 A-I). Arrangement of grains, grain shape, size and pore connectivity in different 2D planes were seen in the images (Figure 5.4A-I; 5.5A-C). Different solid phases are identified in the CT images i.e. heavy minerals, organic matter, fine grains, matrix, pores, fractures etc. Micro- pores are seen in the tomogram (Figure 5.5 B, C). Porosity is computed from resolved pores present in the samples ranging from 3 to 5%.

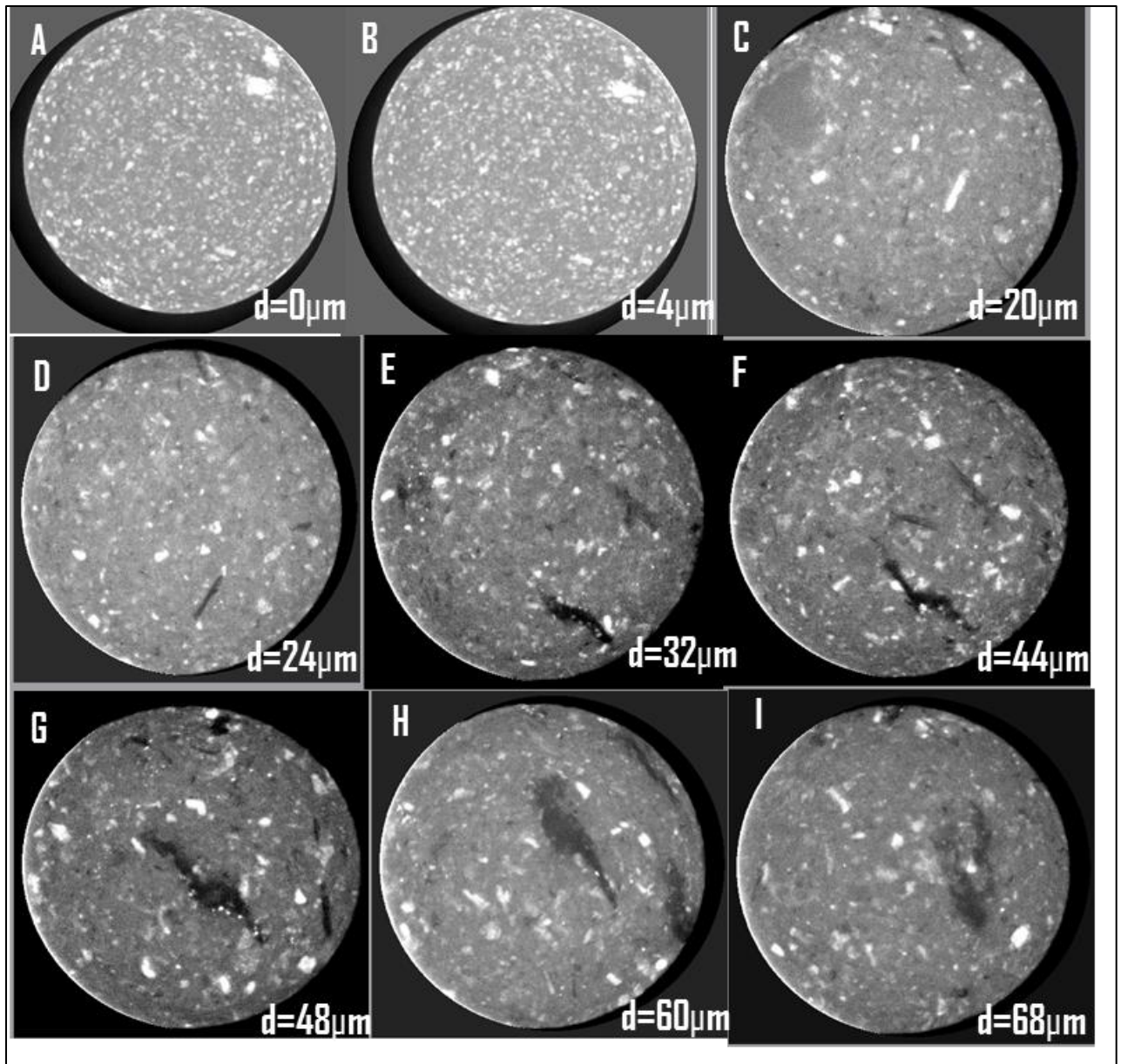


Figure 5.4 CT slices showing the internal heterogeneity of Barren Measures shales, depth 185m; B#1 (d is the distance to the first slice, (A) distribution of grain and matrix; (B) patched of heavy mineral grains at top right corner; (C) finer grains (<50%) with clay matrix, (D) organic matter laths; (E), fracture filled organic matter; (F) and (G) organic matter associated with pores/fracture; (H)&(I) organic matter flakes; here Black to dark black colour is indicating the probable pore and organic matter, grey and white colour are representing the matrix and mineral grains respectively.

b. Identification of natural fractures and fracture orientation

Micro-fractures of varied length and width were identified in the tomograms and segmented images (Figure 5.5 C, D; 5.6A, B, C). The system generated coloured images (2 phases and 3 phases) of samples analyzed to differential grains, matrix and pores + organic matter. The calculated length of the micro- fractures ranges from 0.96mm to 1.42mm at depth 155.1m. The samples were studied in all the planes XY, XZ and ZY. In the segmented images of the sample from 155.1m depth, high density mineral grains (Figure 5.7A) and a thin lamina of high density mineral were observed in XZ plane (Figure 5.7B). The calculated length of the lamina is 2.8mm [Distance of the layer is 694.795 voxel and calculated length is $(694.795 \times 4.03) = 2800.023\mu\text{m}$ i.e. 2.8mm]. The pore space associated with organic matter (Figure 5.8) of almost 8 mm length and 3mm width is identified in the images of the sample from 185m depth. 3D visualization of pore networks of the studied samples were analysed (Figure 5.9A, B, C). In the 3D pore network study, minimum pore and throat radius are resolved up to 0.468 micron where both connected and isolated pores are observed. The most of the pores are with less than 20 micron pore radius and more than 50% of pore throat radius ranges between 10- 20 micron (Figure 5.9D).

c. Porosity measurement and pore network 3D visualization

The most of the pores are isolated and a few micro pores are connected, however the isolated pores may be connected with thin throats of nano scale which were not visible. The different types of pores observed in the images can be classified into three groups: (a) relatively large poorly disconnected pores; (b) large pores connected by very thin conduits; (c) isolated micro pores. As m CT resolved > 0.066 mm of pore, there may be the possibility of presence of pores less than 0.066mm size and also there may be lots of nano pores which are not resolved in these images. Within each of these three categories, the pores are isolated, connected and

partially or completely filled with organic matter and/or detrital clay. Unfortunately, it is very difficult to analyse the presence of features with intermediate attenuation (e.g. clay domains), features like microcracks, micropores and intergranular porosity below image resolution. There may be a significant number of solid/pore-interface voxels leads to an overlap in the density signal. The images show that the samples are moderate to well sorted, grains are sub rounded to rounded which indicate the maturity of the sediments and long distance of provenance.

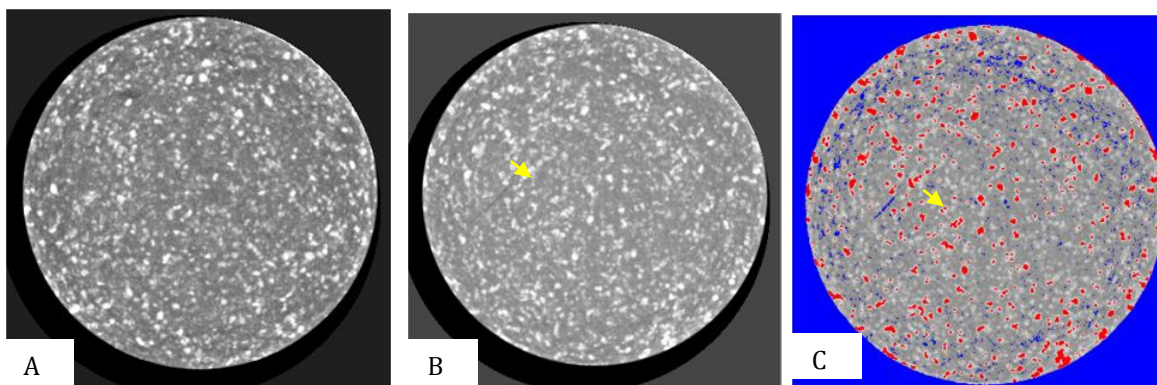


Figure 5.5 Microcomputer tomogram (m CT) images showing pores and microfractures in different Z slices of XY plane. Tomogram showing (A) distribution of grain and matrix; (B) micro fractures, Black to dark black colour is indicating the probable pore and organic matter, grey and white colour are representing the matrix and mineral grains respectively; (C) Analyzed image of a, where Black to dark black colour is indicating the probable pore and organic matter, red colour is indicating relatively higher density mineral grains, grey and white colour are representing the matrix and mineral grains respectively.

Porosity results show that the rock is having poor to moderate reservoir quality. The studied shale samples of Barren Measures shale are highly heterogeneous, moderate to well sorted and tight. The porosity is calculated for the studied m CT images using digital terrain model (Taud, 2005). The computed porosity is 3-5% and porosity values are directly measured based on image pixels. Moreover, the statistical distribution of grain size and porosity were analysed using threshold technique by ImageJ software and a wide range of porosity was

found after analyzing hundreds of slices. In reality higher value of porosity is expected as m CT cannot resolve the nano pores. The Barren Measures shale has complex pore structure and multi scale pore dimensions. The pore diameters of samples vary from a few nano meters to micrometers. The pre-identification of these types of micro- fractures provides significant information about the identification of potential shale gas plays. Therefore nano scale pores were characterized using Transmission Electron Microscope (TEM).

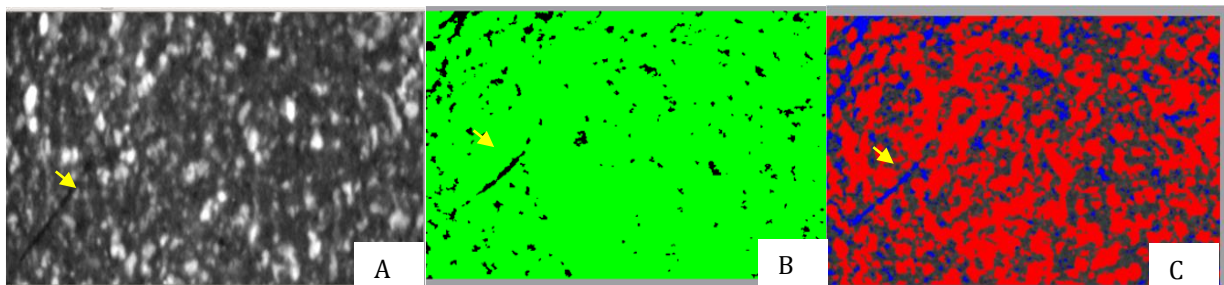


Figure 5.6 Segmented images of tomograms (depth 155m). (A) The fracture is clearly resolved here. (B) The 2 phase analysed images of figure A, black colour indicates pores+ OM and green is grains+ matrix. (C) The three phase segmented image of figure A, red colour is indicating grains, grey is matrix and blue is showing low density areas (pore+ OM).

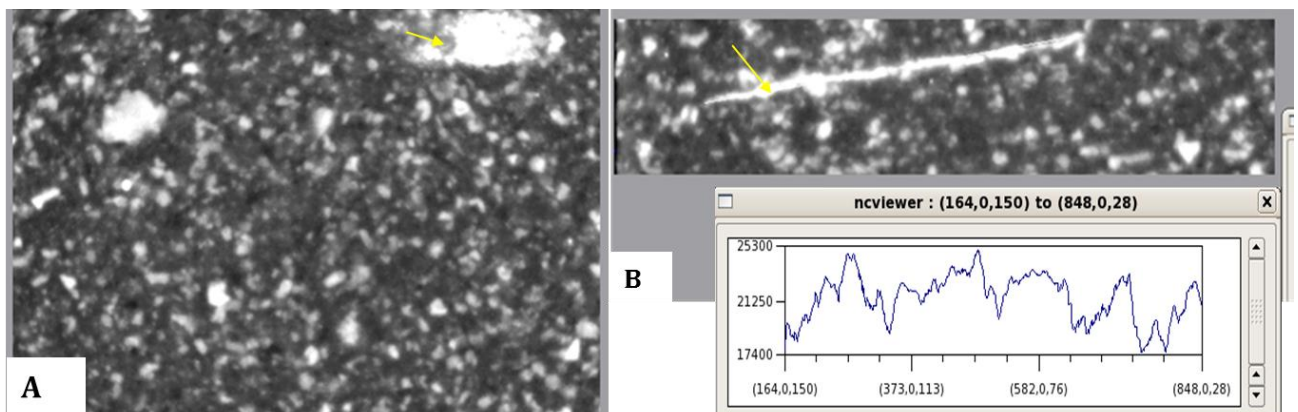


Figure.5.7 Segmented image of Barren Measure shale from 155.1m depth (A) presence of high density mineral grains; (B) a lamina of high density minerals (XZ plane).

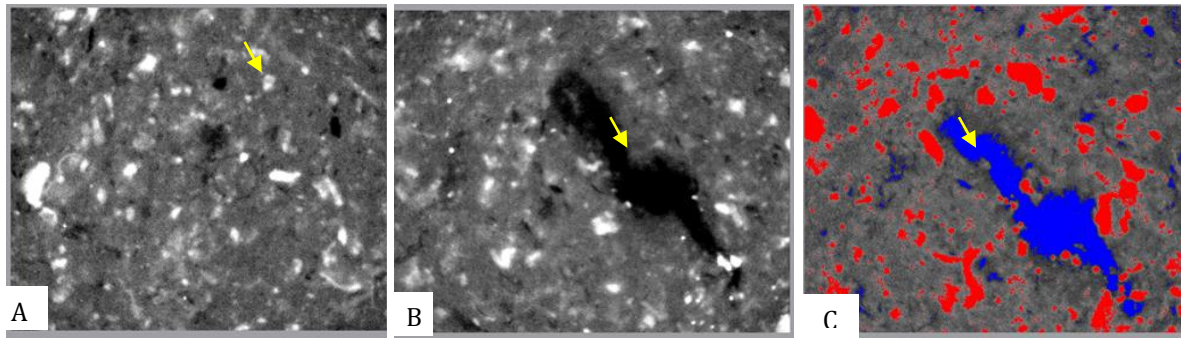


Figure 5.8 Porous space, depth 185m; (A) isolated pores (B) Pores+organic matter at depth 185m. (C) Analyzed image of b indicating the pore space + organic matter by blue colour, matrix with fine grains are by in grey colour and comparatively higher density grains are by red colour.

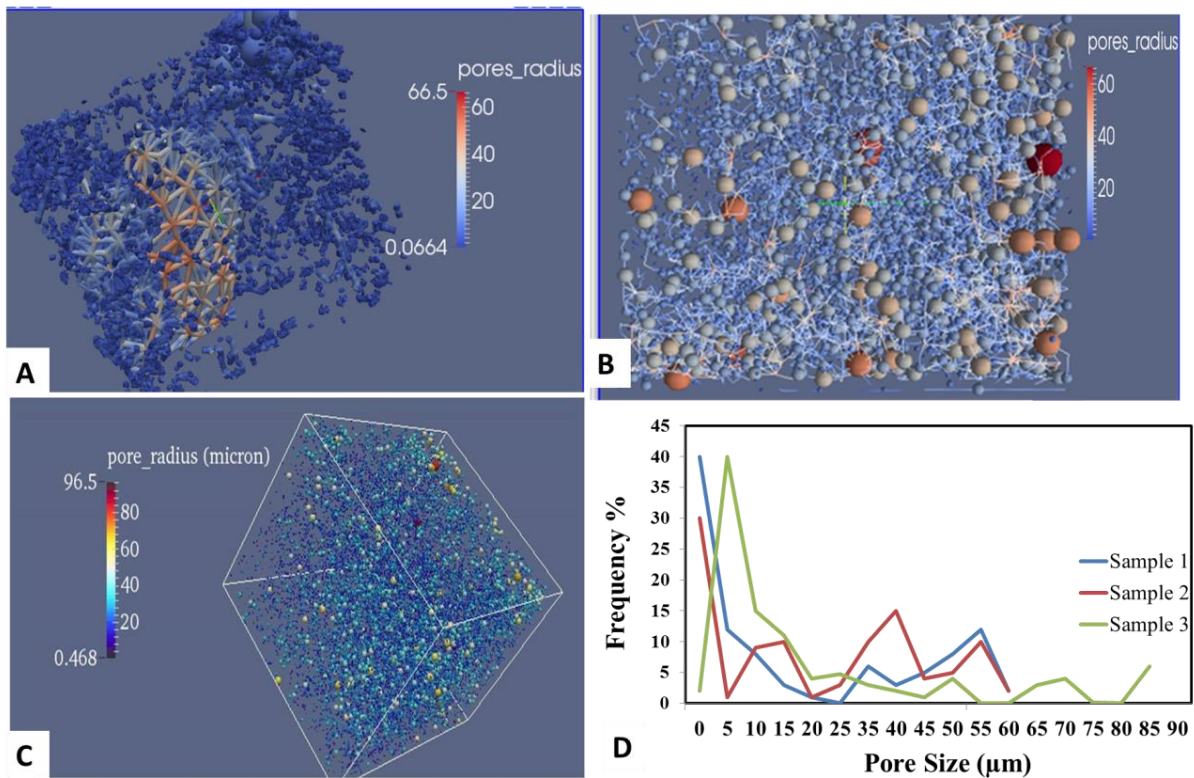


Figure 5.9 3D internal microstructures of Barren Measures shale; (A), (B) & (C) m CT derived 3D image of pore network of samples from the depth of 155m, 155.1m and 185 m respectively. Both isolated and interconnected pore are present. Pore throats are seen to be connected and disconnected. The disconnected pore throats may be either coated with clay or small enough to resolve by the m CT. (D) Pore size distribution graph.

Nano Pores Characterization

The Barren Measures shale is comprised of nano pore which were resolved in Transmission Electron Microscopy (TEM) images. The pores are of different shaped and size ranges from 10nm to 500nm. Interparticle nano pores are clearly visible in the figures (5.10 A-F).

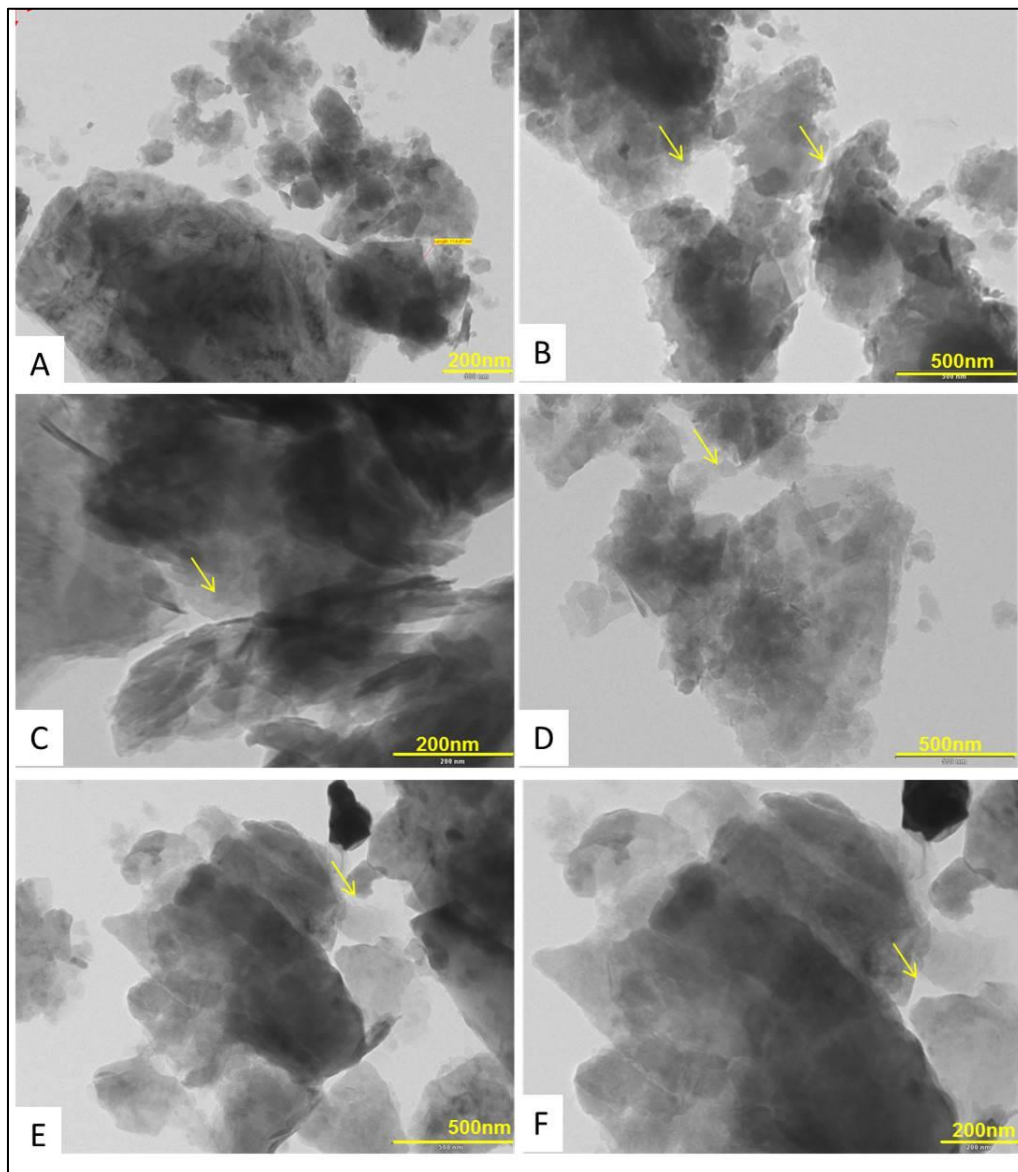


Figure 5.10 TEM images of nano scale pores in Barren Measures shale. A. Interconnected pores with pore throat diameter 110-200nm; intergranular pore spaces of 10-100nm. B. Isolated pores of 200-400nm, intergranular porous spaces of around 50nm; C. Intergranular pores (10-20nm); D. rectangular shaped pores connected with nano pores; E. pore of around 500nm diameter, F. Intergranular pore of around 10nm.

Adsorption Isotherm Analysis Using Brunauer–Emmett–Teller (BET)

In the previous paragraphs, quantitative total porosity analysis and qualitative pore imaging techniques of Barren Measures shale were discussed. Understanding of their pore–size distributions is critical in estimating transport and storage behavior of the shale. Shale exhibits multiple scale pore–structures that are more complex than that of conventional reservoir rocks. In spite of low porosity, shale can hold large quantity of natural in adsorbed state on their internal surfaces. Brunauer–Emmett–Teller (BET) theory is to explain the physical adsorption of gas molecules on a solid surface and effort for the measurement of the specific surface area of shales (Brunauer, Emmett, Teller, 1938). The technique denotes to multi-layer adsorption using non-corrosive gases (like nitrogen, Ar, CO₂ etc.) as adsorbents to define the surface area data. The methane sorption capability, specific surface area and pore size distribution can be quantified using N₂ gas adsorption technique which can examine fine pores in the range of 1.7–200 nm (Ross & Bustin, 2007; Chalmers *et al.* 2012). This experiment was conducted on a Micromeritics ASAP 2010™ instrument. The Micromeritics ASAP 2010 (Accelerated Surface Area and Porosimetry System) offers high quality surface area (BET) and porosity measurement on different types of solid materials based on the gas adsorption theory. Carbon nanotubes and catalysts are characterized using this technique. The Micromeritics ASAP 2010 system consists of an analyzer equipped with two sample preparation ports and one analysis port, a control module, and an interface controller which helps the operation to be controlled easily and accurately. In the analysis port, the free space (dead volume of the tube) is measured volumetrically using helium (reagent grade 99.99% pure) before measurement of the adsorption isotherm. The sample tube, after evacuating the helium, is kept in cryogenic liquid nitrogen (LN₂) treated with a known amount of N₂ at a series of precisely controlled pressures. The gas is allowed to equilibrate with the sample while pressure is examined continuously. When the pressure change per equilibration time

interval (first derivative) is less than 0.01% of the average pressure during the interval, the equilibrium pressure (P) and temperature are noted. The molar quantity of gas adsorbed is calculated by mass balance between the treated amount and the molar quantity of gas in the tube after equilibration. The saturation vapor pressure (P_0) of N_2 at LN_2 temperature is determined every two hours during the experiment using a vapor pressure thermometer.

The quantity of adsorbed gas on the solid surface is measured at discrete pressure (P) steps over the relative equilibrium pressure (P/P_0) range of 0.28518 to 0.973288 at constant temperature. The key assumptions used for reversing the isotherm data to get micropores volume and pore size distribution (PSD) by t-plot and BJH technique, respectively, which is the thickness equation that quantifies the thickness of the adsorbed layer on the pore surface as a function of relative pressure (P/P_0). The shape of the isotherm and its hysteresis pattern provide useful information about the physisorption mechanism. IUPAC (Sing *et al.*, 1985) classified the adsorption isotherms into six types (Type I to VI), along with four hysteresis pattern types (H1 to H4). The different hysteresis patterns H1 to H4 are typical of diverse mesopores shapes. These isotherm types, especially important for unconventional gas (Figure 5.11 & Figure 5.12) are described here. There are also a few mixed Type of isotherm curve such as I/IV and mixed Type II/IV.

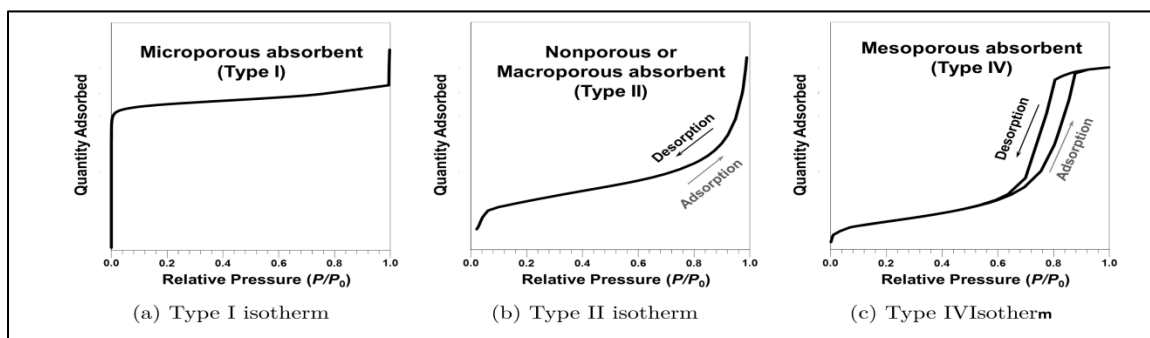


Figure 5.11 Typical isotherm shape exhibited by (a) purely microporous material (Type I isotherm profile) (b) non-porous and macroporous material (Type II isotherm profile) and (c) purely mesoporous materials (Type IV isotherm profile). Modified from Sing *et al.* (1985)

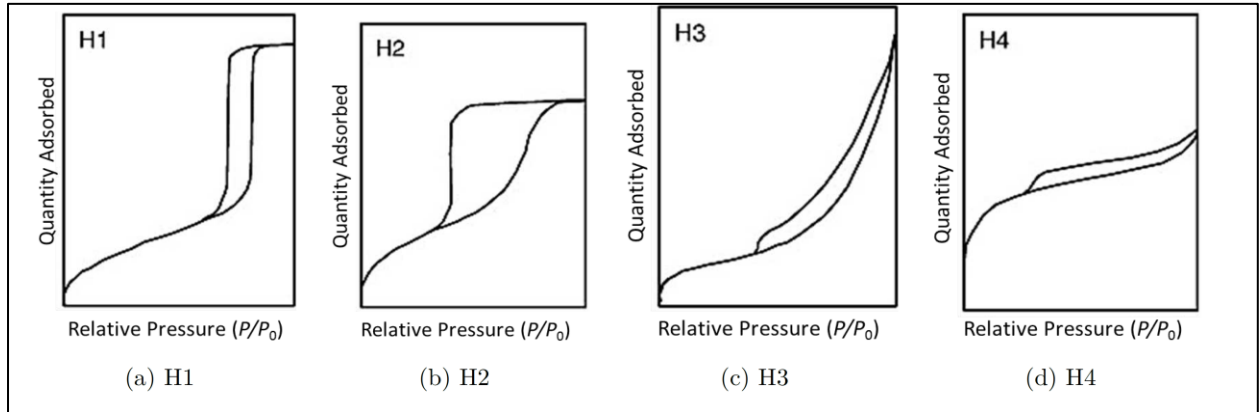


Figure 5.12 The four hysteresis shapes of adsorption isotherm usually found by subcritical N_2 adsorption. Modified from Sing et al. (1985)

The BET analysis was carried out for selective samples of Barren Measures shales and they were Sample 1 (155m depth ; B#1); Sample 2 (170m depth ; B#2), Sample 3 (149m depth ; B#3), Sample 4 (301m depth; B#4). The average surface area, pore sizes and pore volume for all analysed samples are presented in table 5.2.

Table 5.2 Summary results of BET analysis.

Laboratory Investigated Parameters	Sample 1	Sample 2	Sample 3	Sample 4
BET Surface Area:	14.1935	15.1135	11.7592	13.2762
BJH Adsorption Cumulative Surface area of pores(m^2/g)				
Between 17 and 3000 A Diameter(m^2/g)	9.1341	15.0813	9.6205	10.4058
BJH Adsorption Cumulative Surface area of pores				
Between 17 and 3000 A Diameter(m^2/g)	15.8386	0.020716	11.488	13.4603
Volume				
Single Point Adsorption Total Pore Volume of Pores < 744.2342 A Diameter at p/po. 0.97328882(cm^3/g) :	0.025267	0.02071	0.01755	0.018603
BJH Adsorption Cumulative Pore volume of pores Between 17 and 3000 A Diameter(cm^3/g) :	0.022852	0.019349	0.016346	0.017017
BJH Adsorption Cumulative Pore volume of pores Between 17and 3000 A Diameter(cm^3/g) :	0.025716	0.020707	0.17435	0.019625
Pore Size				
Adsorption Avg. Pore Diameter (4V/A by BET) A :	71.2086	54.8342	59.6969	56.0497
BJH Adsorption Avg. Pore Dia (4V/A):	100.0715	60.6717	67.9649	65.4152
BJH Adsorption Avg. Pore Dia(4V/A):	64.945	54.9212	60.7055	58.3199

It results specific surface area of the shale ranges from 11.75m²/g to 15.11 m²/g. The N₂ adsorption isotherm and desorption isotherms for the samples are presented in figure 5.13.

The isotherm are type II for all samples as per BET classification.

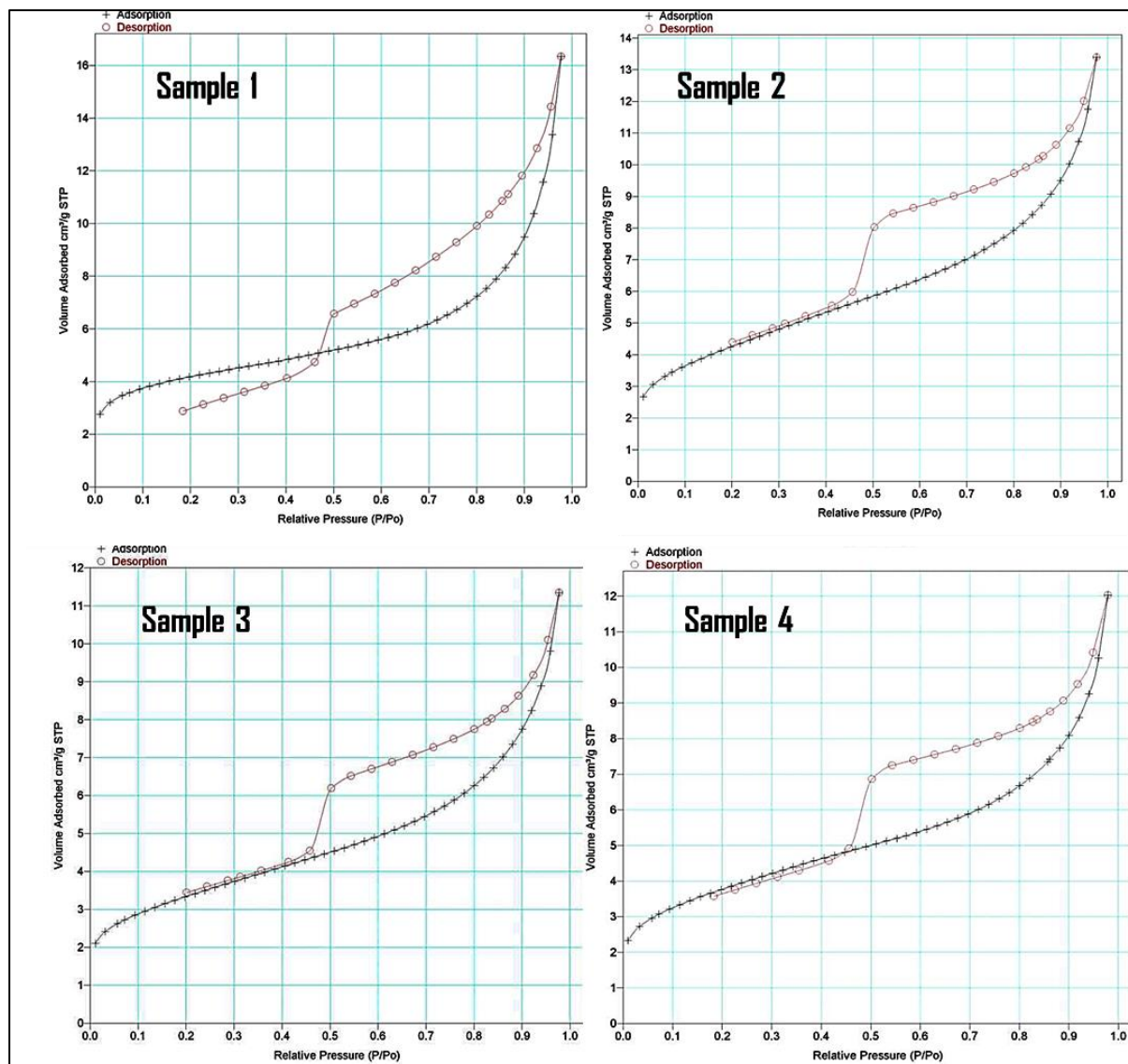


Figure 5.13: N₂ adsorption isotherms at 77K of a representative Barren Measure shale samples. B. figure is showing the isotherm ‘forced closure’ in the relative pressure (P/Po) range 0.48–0.50 due to tensile strength effect.

The significant feature observed in many hysteresis patterns is the forced closure of desorption branch where the isotherm ‘closes’ at P/Po relative pressures around 0.45- 0.50 for N₂ isotherms (Figure 5.13B). This phenomenon is attributed to a process called the Tensile Strength Effect (TSE) (Gregg & Sing, 1983). Loss of the hysteresis is due to the instability of

the hemispherical meniscus during capillary evaporation in pores with diameters smaller than approximately 4 nm. The presence of ‘forced closure’ in the isotherm shape may indicate a significant volume of pores with diameters smaller than 4.5 nm.

The sample 2 is having larger surface area $15.1135\text{m}^2/\text{g}$ followed by sample 1 ($14.193\text{m}^2/\text{mg}$), sample 4 ($13.276\text{m}^2/\text{g}$), sample 3 ($11.759\text{m}^2/\text{g}$). The larger surface area results from the high content of clays, organic matter and very fine grain rock matrix. The studied samples show that the adsorption desorption isotherm curves do not overlap, it results a hysteresis loop. The type is look like to type IV isotherm, caused by capillary condensation in mesopores. The pore size distribution, as interpreted by BJH theory (Figure 5.14) show that the samples 3 and 4 have larger peak at 4nm (40A°) to 10 nm (100A°) while other samples have limited pores below 20nm (200A°) and most of the pores are in the range of 20nm (200A°) to 55nm (550A°). BJH adsorption average pore size diameter ranges from 5.4921nm (54.921A°) to 29.754nm (290.754A°).

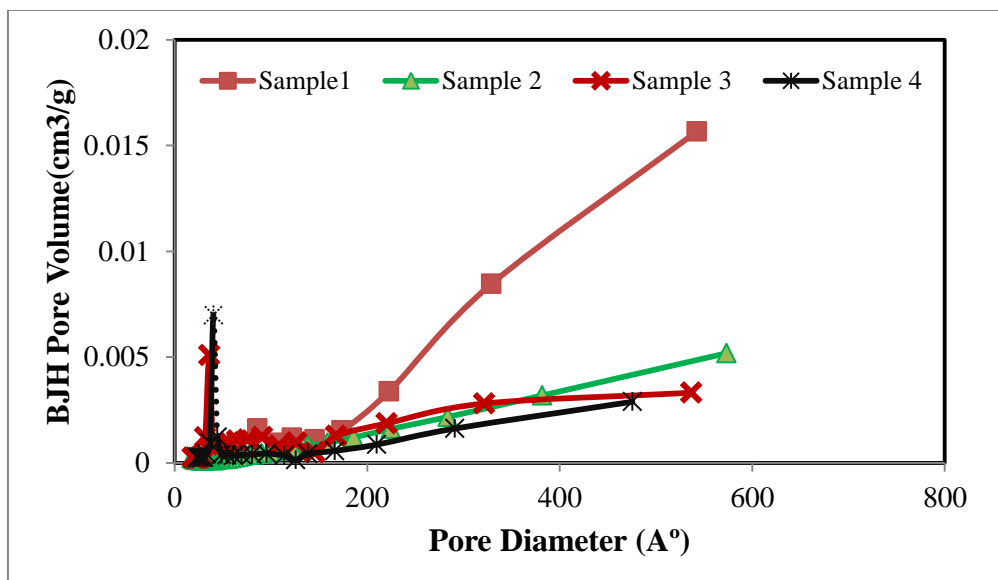


Figure 5.14 BJH Pore size distribution of Barren Measures shale.

In short, the Barren Measures shales are having heterogeneous rock matrix, influenced by: presence of organic Matter, diagenesis effects etc. they have complex pore structure and multi scale pore dimensions. The pore diameters of samples vary from a few nano meters to

